

Effect of Exchanging Advancing and Retreating Side Materials on Mechanical Properties and Electrochemical Corrosion Resistance of Dissimilar 6013-T4 and 7003 Aluminum Alloys FSW Joints

Zhixia Zhao, Haimei Liang, Yong Zhao, and Keng Yan

(Submitted August 20, 2017; in revised form January 7, 2018; published online March 8, 2018)

Friction stir welding (FSW) was used to weld dissimilar joints between Al 6013-T4 and Al7003 alloys in this work. The effect of exchanging advancing (AS) and retreating (RS) side material on microstructure, mechanical behaviors and electrochemical corrosion resistance was discussed. Results showed that different joint cross sections were obtained when exchanging AS and RS materials. The material on the AS would be more deformed during the welding process. When the Al6013 placed on the AS, the plastic flow of weld is more sufficient. Whether on the AS or RS, the Al6013-T4 side is the weak region for both tensile specimens and hardness samples. The fracture position corresponds to the minimum hardness position. Also, more strengthening phase can be retained in the joint, and the joint of A6R7 has better corrosion resistance.

Keywords dissimilar aluminum alloy joints, electrochemical corrosion, friction stir welding, mechanical behavior, microstructure

1. Introduction

Because of its advantages of low density, high strength and good corrosion resistance, aluminum alloy has been widely used in modern industry (Ref 1, 2). However, there are many problems in the use of traditional fusion welding of aluminum alloys, such as the formation of the two brittle phase, the solidification cracking, high deformation, and residual stress (Ref 3).

Friction stir welding (FSW) is a kind of solid state-welding technology, which was invented by the British Welding Research Institute (TWI). In the process of FSW aluminum alloy, the joint does not produce hot cracks, porosity and other fusion welding defects. Therefore, FSW is widely used in aluminum alloy welding (Ref 4-6). Among aluminum alloys, 6xxx and 7xxx aluminum alloys are two of the most widely used aluminum alloys (Ref 7-9).

In recent years, friction stir welding of dissimilar aluminum alloy has been widely studied. Guo et al. (Ref 10) studied the influence of parameters on material flow, microstructure, distribution of micro-hardness and tensile properties of dissimilar aluminum alloy friction stir welding by exchanging materials' location. The researchers studied the distribution of the temperature field, and the effect of the position of the material on the properties had been studied from the macroscopic point of view, but they did not study the mechanism.

Ravikumar et al. (Ref 11) put 6xxx aluminum alloy on the advancing side, and FSW of dissimilar aluminum alloys was carried out at different parameters. The effect of fluidity of materials on the properties of joints was mainly studied. Aval studied the influence of heat input and the natural aging on the residual stress and microstructure of the dissimilar aluminum alloy FSW joint when the 6xxx aluminum alloy was placed on the advancing side (Ref 12), which was mainly focused on the research of micro-components and organizations. Rodriguez et al. (Ref 13) compared the properties of dissimilar aluminum alloys FSW joints and same aluminum alloy FSW joints, and the microstructure and mechanical properties of joints were studied by means of simulation and experiment. Silva et al. (Ref 14) studied the flow and mechanical behavior of the material during the friction stir welding of the dissimilar aluminum alloy and found that the friction stir welding is an asymmetrical welding. Moreover, Giraud et al. (Ref 15) studied microstructure and mechanical properties of dissimilar joint of 7020/6060 aluminum alloys. It found that the position of materials has a significant effect on the microstructure and mechanical properties of joints, but it does not research on the mechanism. According to the literature, influences of sheet configuration on microstructure and mechanical properties of the joints were mainly discussed (Ref 16) and do not involve specific element changes and microscopic mechanisms.

Although there are a lot of researches on friction stir welding of dissimilar aluminum alloys, few people focus on the research of the material on the AS and RS. Friction stir welding is an asymmetrical welding process. The position of the material has a significant influence on the microstructure and properties of the joint when the dissimilar material is welded. Because of the difference of element content, the corrosion resistance of dissimilar aluminum alloy materials will be different. The change of element content at the welded joint of dissimilar aluminum alloy will inevitably lead to potential difference between different regions of the joint, which will affect the corrosion resistance of the joint. In this work, the 6013-T4

Zhixia Zhao, Haimei Liang, Yong Zhao, and Keng Yan, Provincial Key Lab of Advanced Welding Technology, Jiangsu University of Science and Technology, No. 2 Mengxi Road, Zhenjiang 212003 Jiangsu, China. Contact e-mail: yongzhao418@just.edu.cn.

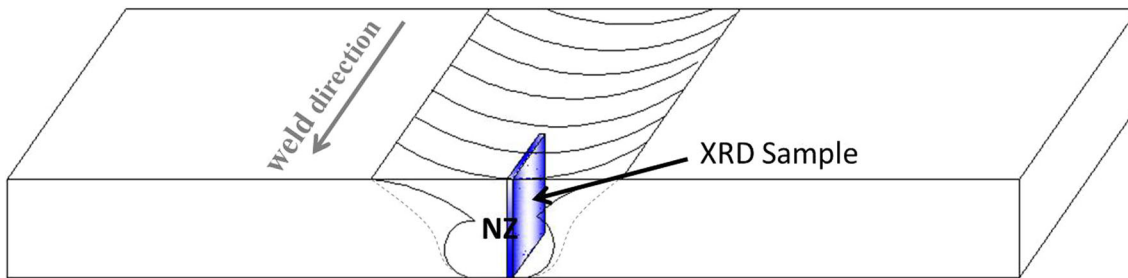


Fig. 1 The location of the XRD test sample

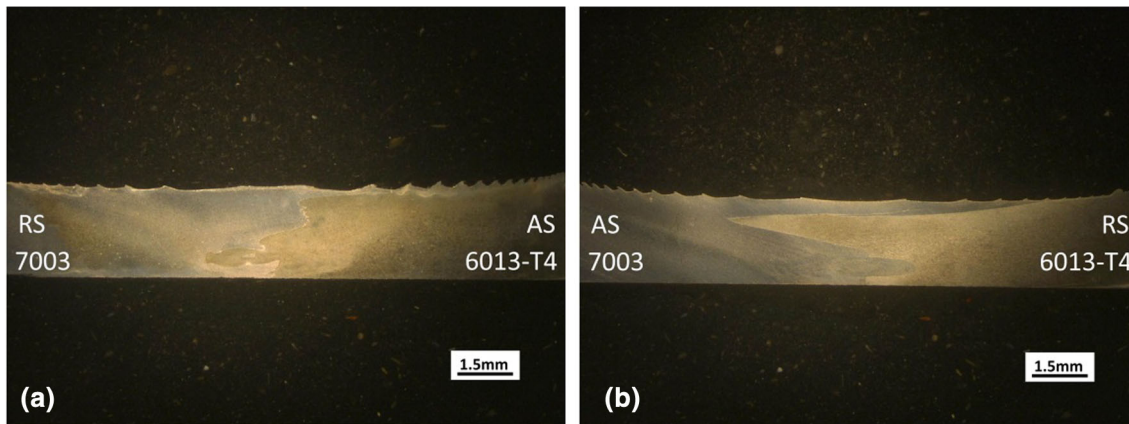


Fig. 2 Macroscopic morphology and fluidity observation of the joints cross section: (a) A6R7 joint. (b) A7R6 joint

aluminum alloy and 7003 aluminum alloy are, respectively, arranged on the AS for FSW. The effect of exchanging AS and RS material on microstructure, mechanical properties and electrochemical corrosion resistance was discussed.

2. Material and Experimental Procedures

The base material (BM) used for the experiment was 6013-T4 aluminum alloy and 7003 aluminum alloy. The dimension of base material is 2.8 mm × 270 mm × 100 mm. The butt joint was adopted. For convenience, the joint which the Al6013-T4 was placed at the advancing side (AS) is called the A6R7 joint. Accordingly, the A7R6 refers to the joint of which the Al7003 was placed at the AS. Before the welding experiment, the surfaces of the sheets were grinded with abrasive paper to remove oxidation films and cleaned with alcohol. FSW tool was made of 9341 tool steel. The shoulder diameter of the tool was 16 mm. The pin of the tool consists of a conic shape (with the maximum diameter of 4.9 mm and the minimum diameter of 3.84 mm) and a length of 2.5 mm. During FSW, rotation speed of tool was 800 rpm and welding speed was 400 mm/min. Tilt angle of the tool axis was 2.5° during the experiment.

After welding, the metallographic specimens were etched with Keller's reagent (2 ml HF + 3 ml HCl + 5 ml HNO₃ + 190 ml distilled water) and observed by optical microscopy (OM). ASME BPVC Section IX-2015 was followed in preparing the tensile specimens. Tensile test was carried out by CMT5205 tensile testing machine. Scanning electron

microscope and energy-dispersive spectrometer (SEM-EDS) were used to observe the fracture morphology, and x-ray diffraction (XRD) was used in determining strengthening precipitates in joints. The XRD test samples are parallel to the weld direction and cut out at the nugget region. The sampling position is shown in Fig. 1. The micro-hardness measurement was applied to cross section of joint by MH-5D hardness tester (load 200 g, time 5 s). The location of the test points is 1 mm from the distance surface. Electrochemical corrosion test was conducted in electrochemical work station with EG&G PARV M283 potentiostat and 1025 lock-in amplifier. Saturated calomel electrode (SCE) worked as reference electrode, and platinum was auxiliary electrode. The electrochemical corrosion test samples are parallel to the weld direction which cut out at the nugget region. The all the electrodes were dipped in 3.5% NaCl solution for 30 min when the circuit was connected.

3. Results and Discussion

3.1 Morphology of Joints

Figure 2 shows the macrographs of joints welded by FSW when the Al7003 and Al6013 were placed on AS, respectively. The dividing line between two kinds of aluminum alloy can be seen from the macroscopic view. The Al6013-T4 alloy features as darker colors, while Al7003 alloy features as light color which is because of their different etching response to the Keller's reagent.

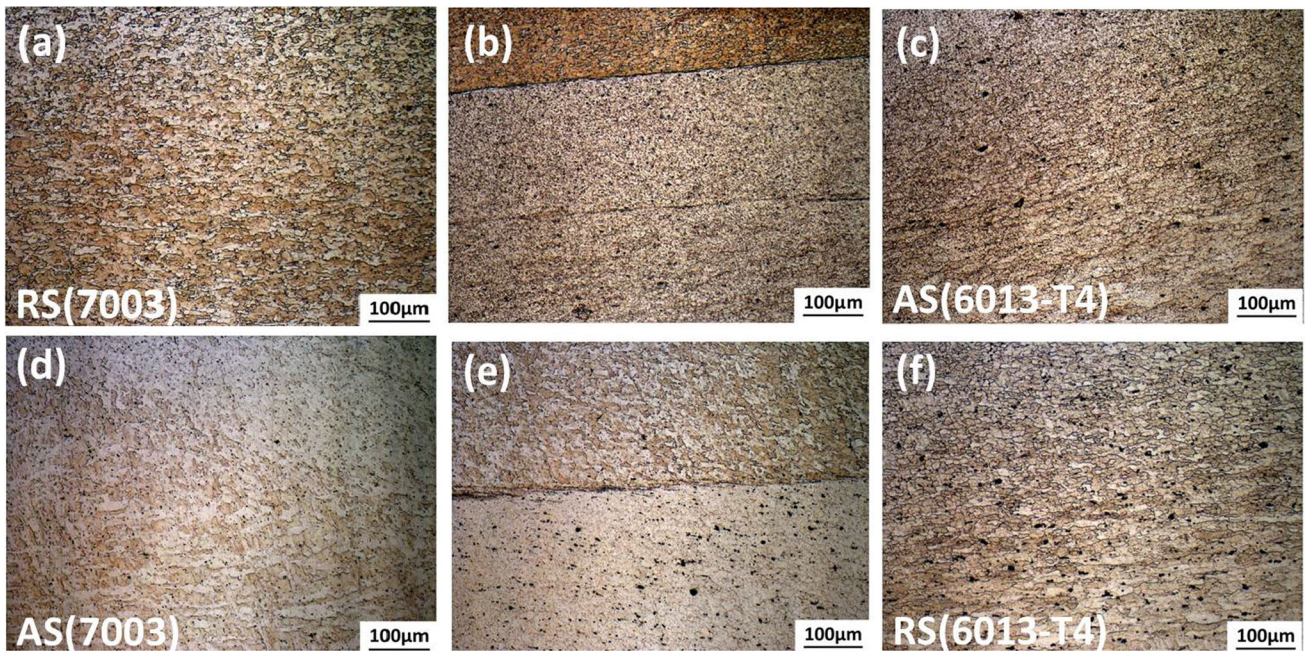


Fig. 3 Microstructures in each region of the joints: (a) TMAZ on the AS, (b) SZ and (c) TMAZ on the RS of A6R7 joint; (d) TMAZ on the AS, (e) SZ and (f) TMAZ on the RS of A7R6 joint

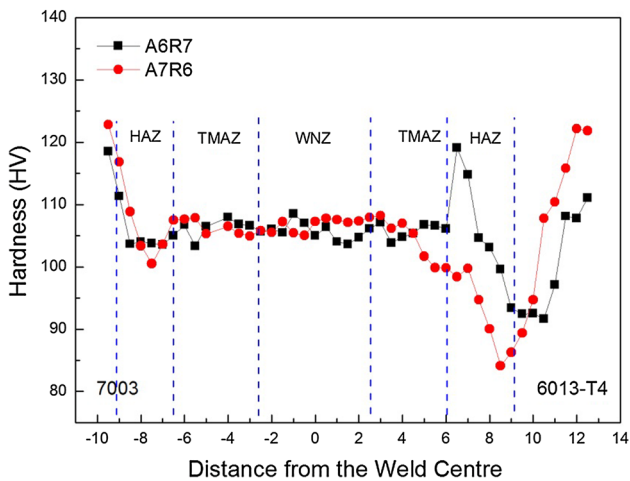


Fig. 4 Micro-hardness test results of the joints cross section

From these macrographs, it can be seen that the stir zones (SZ) of the joints present tapered morphologies due to the pin shape. Interfaces between the thermal-mechanically affected zone (TMAZ) and the SZ can be clearly recognized. It is evident that sound joints of 6013-T4-7003 Al alloys were achieved under all the investigated welding conditions. The two aluminum alloys in the weld are not fully blended even after severe agitation, especially on the RS. When changing the materials location, very different material flow behaviors can be formed. It seems that the material mixed more fully in the A7R6 joint (Fig. 2b). But the bonding interface is very sharp. For the A6R7 joint (Fig. 2a), relative smooth bonding interface can be observed. This difference is more evident which mainly reflects the internal weld metal fluidity. During welding, basic materials properties have an important effect on material flow behavior. It is obvious that the Al6013-T4 alloy has better plastic flow properties than Al7003 alloy. For the A7R6 joint,

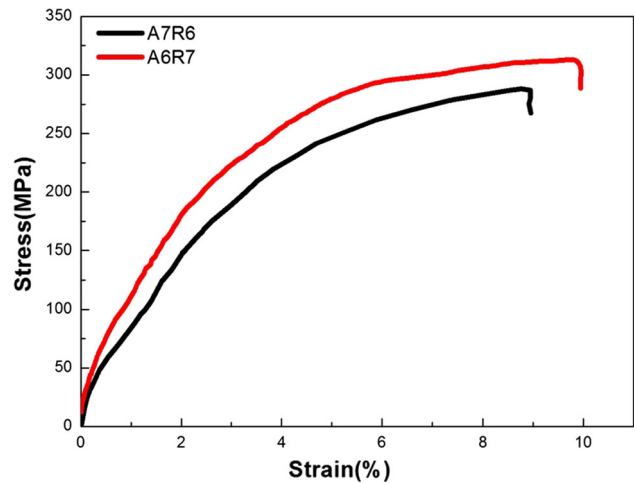


Fig. 5 Stress-strain curves of tensile specimens

the material flow resistance at the RS is relatively small. More violent material flow can be obtained, and hence, part of the Al6013-T4 alloy flows into the AS. For the A6R7 joint, big material flow resistance at the RS causes the material at RS more difficult to flowing to the AS. Hence, no Al7003 alloy can be observed at the AS.

3.2 Microstructure of Joints

Figure 3 shows the microstructure of the joints. Figure 3(a), (b), and (c) shows the microstructure of the A6R7 joint. Figure 3(d), (e), and (f) shows the microstructure of the A7R6 joint. The grain size in Fig. 3(d) is obviously larger than that in Fig. 3(a), and the size in Fig. 3(c) is larger than that in Fig. 3(f). At the same time, the material on the AS has a severe deformation in the TMAZ, compared to the material located in the RS. In the process of FSW, the heat at the AS is higher,

which makes the grain size become coarse. It indicates that the heat produced at the AS is more than that produced at the RS in the FSW process. It can be seen that many black spots appear in the microstructure of the A7R6 joint, especially the TMAZ on the RS of A7R6 joint. This black spot rarely occurs at A6R7 joint. This shows that when the Al6013-T4 placed on the AS of the welding, the joints are not easy to precipitate strengthening phase.

3.3 Micro-hardness

Figure 4 shows the result of micro-hardness test, and it reveals the soften zone in both joints. It can be seen no softening occurred on side of the Al7003. On the both joints, the minimum hardness locates at the HAZ region at the Al6013-T4 side. The A7R6 joint minimum hardness is 84.5 HV. The hardness on the HAZ is higher at 6013-T4 side when it put on the AS.

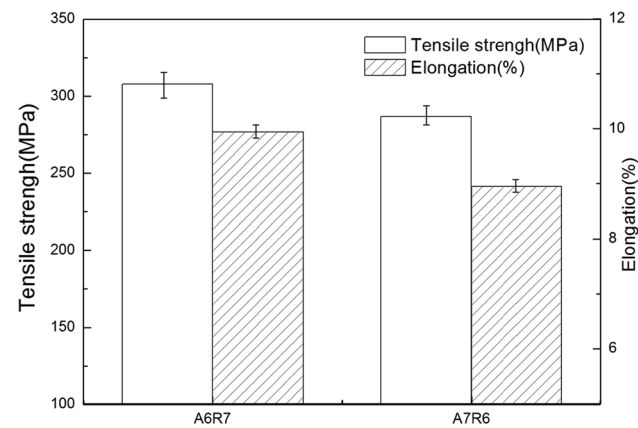


Fig. 6 Results of tensile test: tensile strength and elongation of joint

In the HAZ, finely strengthening phase aggregates when the temperature is low which leads to over aging in this area. Corresponding to Fig. 3, a lot of precipitated phases are precipitated in the HAZ on the Al6013 side. This is the reason for the reduction of joint strength and micro-hardness. Al7003 is rolling state, and the phase precipitated in the HAZ during the welding process. The hardness of the Al7003 is lower than that of the BM, but the hardness is higher than the Al6013 side because of the rolling state before the welding.

3.4 Mechanical Properties

Figure 5 illustrates the stress–strain curves of joints. Based on the stress–strain curves, the tensile strength and elongation were calculated and presented as shown in Fig. 6. The tensile strength of joint A6R7 is 308 MPa, which is approximately 93% of base metal strength. The joint A7R6 had an ultimate tensile strength of

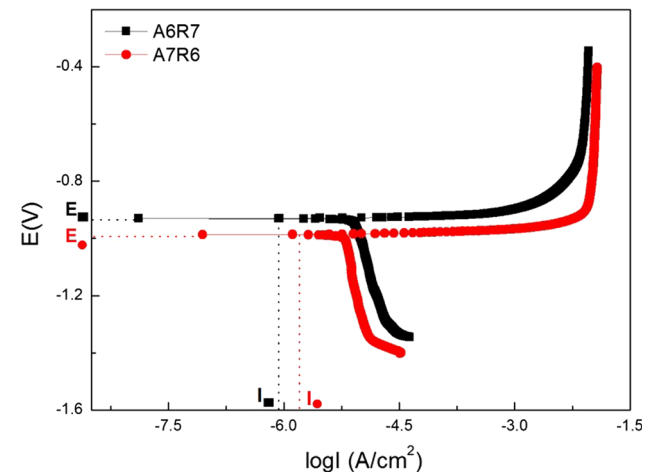


Fig. 8 Tafel curves of samples

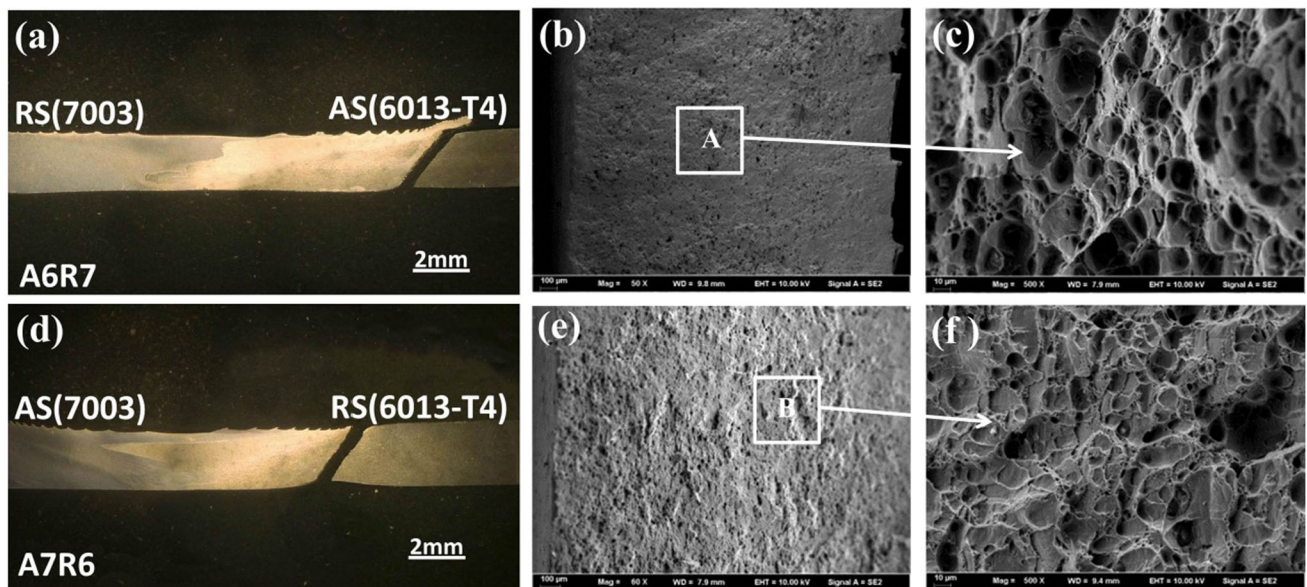
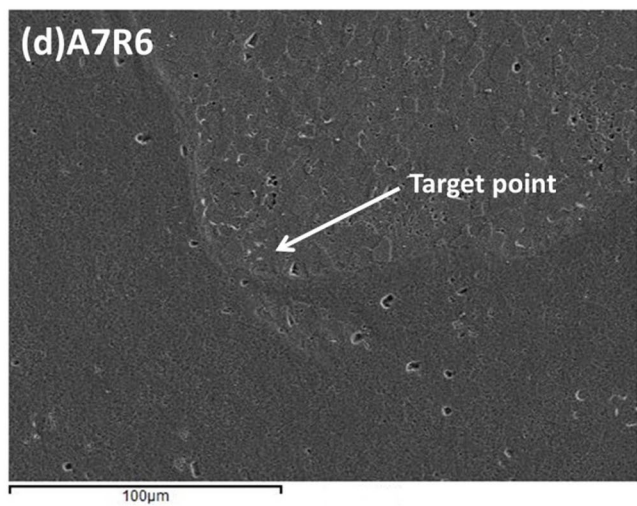
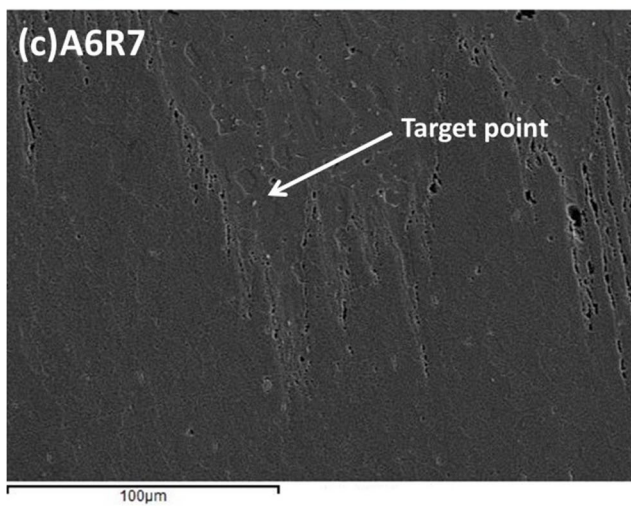
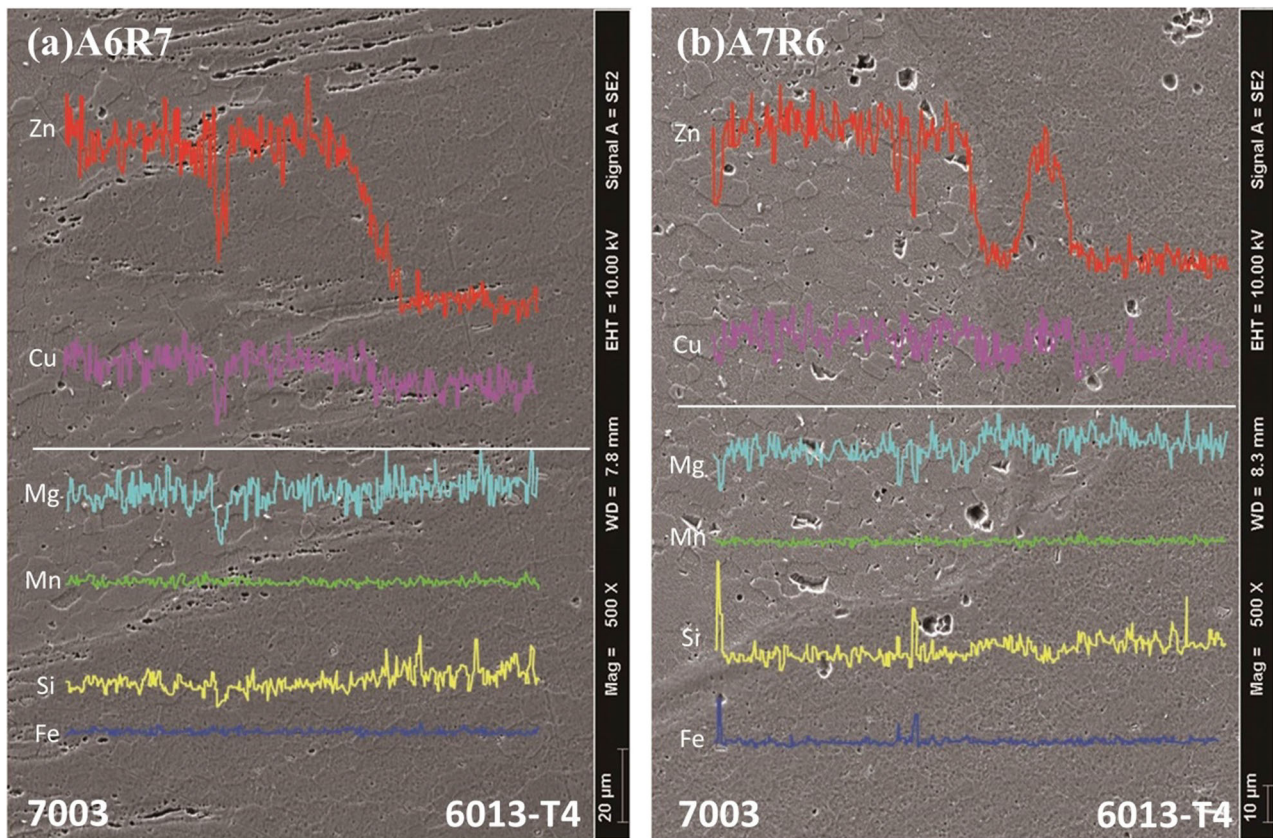


Fig. 7 (a) Fracture position of the A6R7 joint, (b) the fracture macroscopic morphology of the A6R7 joint, (c) micromorphology of fracture (amplification of the A position), (d) fracture position of the A7R6 joint, (e) the fracture macroscopic morphology of the A7R6 joint, (f) micromorphology of fracture (amplification of the B position)



Element	Weight(%)	Atom(%)
Al K	93.21	95.46
Mg K	1.06	1.19
Si K	0.33	0.32
Zn K	3.03	2.01
Cu K	2.37	1.02
Total	100.00	100.00

Element	Weight(%)	Atom(%)
Al K	91.43	94.33
Mg K	1.02	1.17
Si K	1.05	0.71
Zn K	2.15	1.89
Cu K	4.35	1.90
Total	100.00	100.00

Fig. 9 Results of SEM and EDS at SZ center of the joints: (a) line scan of joint A6R7, (b) line scan of joint A7R6, (c) component analysis at SN of A6R7 joint, (d) component analysis at SN of A7R6 joint

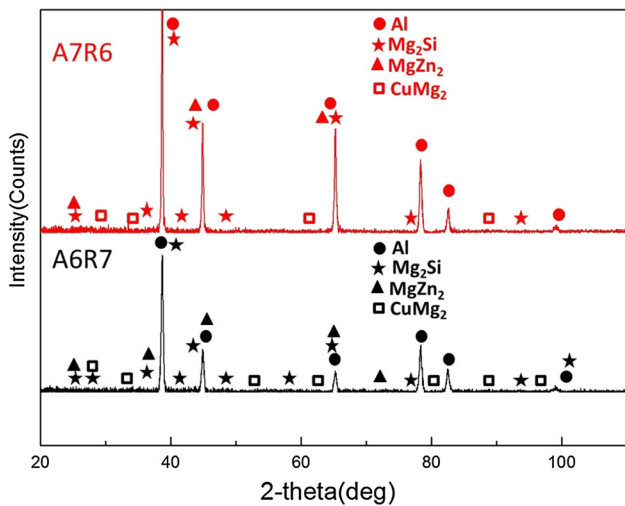


Fig. 10 Analysis of XRD spectra

287 MPa, equivalent to 87% of base metal strength. The A6R7 joint had better plastic, elongation of which is 9.9%.

Figure 7 is the schematic diagram of tensile fracture position of welded joint. It can be seen that the joints fractured at 45 degrees angle. All of these fracture positions are the HAZ at the side of Al6013-T4. No matter the joint A6R7 or A7R6, the side of Al6013-T4 is weak zone. The fracture position corresponds to the minimum hardness position. Observing by the electron microscope, it can be seen that there are dimples in the fracture of the two joints. The fracture surfaces of A6R7 had many small and dense dimples, while the dimples on the A7R6 fracture surfaces are relatively small and shallow. These characteristics show that the fracture forms of the two joints are ductile fracture, and the strength and plasticity of the A6R7 joint are higher. This result agrees with the result of the tensile test.

3.5 Corrosion Resistance

Tafel curves are shown in Fig. 8. Corrosion rate is in proportion to corrosion current (I_{corr}) (Ref 17). As can be seen from the Fig. 6, the corrosion current of A7R6 joint ($I_{\text{corr}} = -5.8 \text{ A/cm}^2$) is larger, so the corrosion rate of A7R6 joint is faster. Corrosion potential (E_{corr}) reveals corrosion tendency, and the more positive it is the harder corrosion initiates (Ref 18). The corrosion potential of A6R7 joint ($E_{\text{corr}} = -0.93 \text{ V}$) is larger than the corrosion potential of A7R6 joint ($E_{\text{corr}} = 0.99 \text{ V}$), so it is difficult for A7R6 to corrode. Under the same welding parameters, the corrosion point is lower and the corrosion current density is lower when the Al6013 alloy is placed on AS. As a consequence, the weld has better corrosion resistance when Al6013 alloy is placed on the advancing side of the weld.

3.6 Phase and Element Analysis

SEM-EDS analysis and XRD spectra of A6R7 joint and A7R6 joints are displayed in Fig. 9 and 10, respectively. Figure 9(a) and 10 show the results of line scan of joint A6R7 and A7R6, respectively. Cu, Mg, Mn and Fe element distribution shows little difference at two sides of the bonding interface. For the Zn and Si elements, especially Zn, obvious gradient can be seen at the bonding interface. The uneven elements distribution may affect

the joint mechanical properties and electrochemical corrosion resistance. Figure 9(c) and (d) shows the results of the element scan of the joints A6R7 and A7R6, respectively. Some special points could be seen in the SEM map of samples, and these points were supposed to be the strengthening precipitation. The content analysis of component shows that the content of Zn element decreases at the bonding interface of A7R6 joint and Si element has precipitation. The Cu element was obviously affected, and precipitation occurred. The distribution of elements in the joint and the amount of precipitation will affect the phase transformation in the joint, which further influences the properties of the joint. According to the analysis of SEM-EDS, the elements in the joint A6R7 gradually changed at the bonding interface. And the Cu element in the joint A6R7 has less melting off. The strengthening phase can be preserved more in the joint A6R7.

The strengthening phase in base metal of Al6013-T4 is Mg_2Si , and the strengthening phase in Al7003 alloy is MgZn_2 . XRD analysis indicated that strengthening phases in both joints were Mg_2Si , MgZn_2 and CuMg_2 . Al7003 is affected by excessive heat on AS, so the Zn and Cu elements are more precipitated. And the number of MgZn_2 and CuMg_2 peaks in the XRD spectrum of the joint A7R6 decreased. The MgSi_2 phase remains a lot although it is over aging. The number of peaks decreasing affects the tensile properties of the joint. This is the reason that the tensile strength and elongation of the joint A7R6 are less than the joint A6R7.

The variation in strengthening phases resulted in complex corrosion behavior of joints. Former study (Ref 19, 20) shows that the potential of MgZn_2 in the grain is -0.87 V and the potential of Mg_2Si particles is about -1.54 V in NaCl solution. The potential of Mg_2Si is lower than the matrix and the other zone without precipitation, so Mg_2Si works as anode and it was easy to be corroded. The corrosion potential of the sample A6R7 is the highest. According to the XRD spectra, when the Al6013-T4 puts on AS, Mg_2Si is relatively small, which is because the heat generated at AS is relatively high, resulting in Mg_2Si dissolution. When Al7003 is placed on the AS, the corrosion resistance of the weld is poor, the reason is that the Mg_2Si phase is less, while the MgZn_2 dissolves more.

4. Conclusions

In the present study, FSW was used to fabricate Al6013-T4 and Al7003 aluminum alloys joint. The effect of exchanging forward and backward side materials on microstructure, mechanical behaviors and electrochemical corrosion resistance was mainly discussed. The main conclusions can be summarized as follows:

1. Both joints, A6R7 or A7R6, can be welded without defects. When exchange the AS and RS materials, different cross sections can be obtained. More fully mixed joint can be obtained when Al6013-T4 put at AS. A6R7 joint retained much precipitate strengthening.
2. The Al6013-T4 side is the weak region for tensile specimens. The tensile specimens were broken on the Al6013-T4 side, both of which were ductile fracture. Whether on the AS or RS, the Al6013-T4 side is the weak region for hardness samples.

- Strengthening phase retained in the A6R7 joint, which has better corrosion resistance. The joint A7R6 is not only easy to corrosion, but once the corrosion began, the rate of corrosion is still faster.

References

- F.F. Wang, W.Y. Li, J. Shen, S.Y. Hu, and J.F.D. Santos, Effect of Tool Rotational Speed on the Microstructure and Mechanical Properties of Bobbin Tool Friction Stir Welding of Al-Li Alloy, *Mater. Des.*, 2015, **86**, p 933–940
- S.D. Ji, Y.Y. Jin, Y.M. Yue, S.S. Gao, Y.X. Huang, and L. Wang, Effect of Temperature on Material Transfer Behavior at Different Stages of Friction Stir Welded 7075-T6 Aluminum Alloy, *J. Mater. Sci. Technol.*, 2013, **29**(10), p 955–960
- B.T. Gibson, D.H. Lammlein, T.J. Prater, W.R. Longhurst, C.D. Cox, M.C. Ballun, K.J. Dharmaraj, G.E. Cook, and A.M. Strauss, Friction Stir Welding: Process, Automation, and Control, *J. Mater. Process. Technol.*, 2014, **16**(1), p 56–73
- S.J. Chen, Y. Zhou, J.R. Xue, R.Y. Ni, Y. Guo, and J.H. Dong, High Rotation Speed Friction Stir Welding for 2014 Aluminum Alloy Thin Sheets, *J. Mater. Eng. Perform.*, 2017, **26**, p 1–9
- S.J. Chen, H. Li, S. Lu, R.Y. Ni, and J.H. Dong, Temperature Measurement and Control of Bobbin Tool Friction Stir Welding, *Int. J. Adv. Manuf. Technol.*, 2015, **86**(1–4), p 1–10
- S.J. Chen, H. Li, M. Wu, J.R. Xue, and J.H. Dong, Torque Oscillation Characteristics in the Process of Bobbin Tool Friction Stir Welding, *J. Vibroeng.*, 2016, **18**(1), p 70–80
- S. Lu, X.D. Jia, C.Y. Zhang, J.J. Gong, L. Fu, and X.Y. Dong, Temperature Field and Microstructure of Magnesium Alloy Fabricated by FSW, *J. Mater. Eng.*, 2009, **1**, p 9–13
- W.M. Thomas, E.D. Nicholas, J.C. Needham, M.G. Murch, P. Templesmith, and C.J. Dawes, Friction-Stir Butt Welding. G.B. Patent 9125978.8, UK, 1991
- P.A. Schweitzer, Aluminum and Aluminum Alloys, *Met. Mater. Phys. Mech. Corros. Prop.*, 2003, <https://doi.org/10.1201/9780203912423.ch19>
- J.F. Guo, H.C. Chen, C.N. Sun, G. Bi, Z. Sun, and J. Wei, Friction Stir Welding of Dissimilar Materials Between AA6061 and AA7075 Al Alloys Effects of Process Parameters, *Mater. Des.*, 2014, **56**, p 185–192
- S.R. Kumar, V.S. Rao, and R.V. Pranesh, Effect of Welding Parameters on Macro and Microstructure of Friction Stir Welded Dissimilar Butt Joints between AA7075-T651 and AA6061-T651 Alloys, *Procedia Mater. Sci.*, 2014, **5**(1), p 1726–1735
- H.J. Aval, Microstructure and Residual Stress Distributions in Friction STIR Welding of Dissimilar Aluminum Alloys, *Mater. Des.*, 2015, **87**, p 405–413
- H.J. Aval, S. Serajzadeh, and A.H. Kokabi, Evolution of Microstructures and Mechanical Properties in Similar and Dissimilar Friction Stir Welding of AA5086 and AA6061, *Mater. Sci. Eng. A*, 2011, **528**(28), p 8071–8083
- A.A.M.D. Silva, E. Arruti, G. Janeiro, E. Aldanondo, P. Alvarez, and A. Echeverria, Material Flow and Mechanical Behaviour of Dissimilar AA2024-T3 and AA7075-T6 Aluminium Alloys Friction Stir Welds, *Mater. Des.*, 2011, **32**(4), p 2021–2027
- L. Giraud, H. Robe, C. Claudin, C. Desrayaud, P. Bocher, and E. Feulvarchet, Investigation into the Dissimilar Friction Stir Welding of AA7020-T651 and AA6060-T6, *J. Mater. Process. Technol.*, 2016, **235**, p 220–230
- S.K. Park, S.T. Hong, J.H. Park, K.Y. Park, Y.J. Kwon, and H.J. Son, Effect of Material Locations on Properties of Friction Stir Welding Joints of Dissimilar Aluminum Alloys, *Sci. Technol. Weld. Join.*, 2010, **15**(4), p 331–336
- K.G. Conroy and C.B. Breslin, The Electrochemical Deposition of Polyaniline at Pure Aluminum: Electrochemical Activity and Corrosion Protection Properties, *Electrochim. Acta*, 2003, **48**(6), p 721–732
- X.C. Liu, C.Q. An, and Z.X. Cui, *Metal Corrosion*, 4th ed., National Defence Industry Press, Beijing, 2002
- Z.T. Wang and R.Z. Tian, *Handbook of Aluminum Alloy and its Working*, 2nd ed., Central South University Press, Changsha, 2000
- F.L. Zeng, Z.L. Wei, J.F. Li, C.X. Li, X. Tan, Z. Zhang, and Z.Q. Zheng, Corrosion Mechanism Associated with MgSi and Si Particles in Al-Mg-Si Alloys, *Metal. Soc.*, 2011, **21**(12), p 2559–2567